Molecular Therapy
Oncolytics
Original Article

The NRF2-dependent transcriptional axis, XRCC5/hTERT drives tumor progression and 5-Fu insensitivity in hepatocellular carcinoma

Tianze Liu,[1,2,3,6] Qian Long,[1,6] Luting Li,[3,4,6] Hairun Gan,[3,4,6] Xinyan Hu,[3,4] Haoyu Long,[3,4] Lukun Yang,[5] Pengfei Pang,[3,4] Siyang Wang,[2] and Wuguo Deng[1]

[1]Sun Yat-sen University Cancer Center, State Key Laboratory of Oncology in South China, Collaborative Innovation Center of Cancer Medicine, Guangzhou 510060, China; [2]The Cancer Center of The Fifth Affiliated Hospital Sun Yat-sen University, Zhuhai 519000, China; [3]Guangdong Provincial Key Laboratory of Biomedical Imaging and Guangdong Provincial Engineering Research Center of Molecular Imaging, Zhuhai 519000, China; [4]Department of Interventional Medicine, The Fifth Affiliated Hospital of Sun Yat-sen University, Zhuhai 519000, China; [5]Department of Anesthesiology, The Fifth Affiliated Hospital of Sun Yat-sen University, Zhuhai 519000 China

Human telomerase reverse transcriptase (hTERT) is highly expressed in many tumors and is essential for tumorigenesis and metastasis in multiple cancers. However, the molecular mechanisms underlying its high expression level in hepatocellular carcinoma (HCC) remain unclear. In this study, we identified X-ray repair cross-complementing 5 (XRCC5), a novel hTERT promoter-binding protein in HCC cells, using biotin-streptavidin-agarose pull-down assay. We found that XRCC5 was highly expressed in HCC cells, in which it transcriptionally upregulated hTERT. Functionally, the transgenic expression of XRCC5 promoted HCC progression and 5-fluorouracil resistance, whereas short hairpin RNA knockdown of XRCC5 had converse effects *in vitro* and *in vivo*. Moreover, hTERT overexpression reversed XRCC5 knockdown- or 5-fluorouracil (5-Fu)-mediated HCC inhibition. Mechanistically, nuclear-factor-erythroid-2-related factor 2 (NRF2) interacted with XRCC5, which in turn upregulated hTERT. However, the upregulation was insignificant when NRF2 was reduced, suggesting that the XRCC5-mediated hTERT expression was NRF2 dependent. The HCC patients with high expression levels of XRCC5 and hTERT had shorter overall survival times compared with those with low XRCC5 and hTERT levels in their tumor tissues. Collectively, our study demonstrates the molecular mechanisms of the XRCC5/NRF2/hTERT signaling in HCC metastasis, which will aid in the identification of novel strategies for the diagnosis and treatment of HCC.

INTRODUCTION

Hepatocellular carcinoma (HCC), a solid malignant tumor fairly common in humans, is currently the third leading cause of cancer deaths worldwide.[1,2] In many developed countries, the incidence and mortality of HCC shows an ascendant trend, with approximately 750,000 people dying from the disease annually.[3,4] Owing to the subtle clinical presentations, more than 60% of HCC patients are diagnosed at an advanced stage.[5] Despite recent advances in the diagnosis and treatment of HCC, the 5-year survival rate of HCC patients remains unsatisfactory.[6] Therefore, there is an urgent need to identify more effective therapeutic targets for the treatment of HCC.

Human telomerase reverse transcriptase (hTERT), the catalytic subunit of telomerase, caps the ends of eukaryotic chromosomes with telomeres, which are associated with genome stability and chromosome integrity for long-term proliferation.[7–9] Given that the germline reduction in telomerase function leads to telomere biology disorders (TBDs), an optimum level of hTERT expression is required for tissue homeostasis.[9] Importantly, more than 90% of all human tumors are characterized by hTERT-mediated upregulation of telomerase activity.[10,11] Recently, numerous studies have established the strong positive correlation between the activation and relatively high expression level of hTERT and oncogenesis and proposed hTERT as a molecular marker for tumors. However, the molecular mechanisms underlying the high expression level of hTERT in HCC remain unclear. Therefore, we explored the molecular mechanisms underlying the tumor-specific expression and activation of hTERT.

The Ku protein, composed of the Ku70 (X-ray repair cross-complementing 6 [XRCC6]) and Ku80 (XRCC5) polypeptides, is a highly conserved DNA-binding protein playing crucial roles in the maintenance of chromosome stability.[12] Previous studies have reported that Ku80 is recruited during DNA double-strand break (DSB) repair and

Received 1 March 2021; accepted 17 December 2021;
https://doi.org/10.1016/j.omto.2021.12.012.

[6]These authors contributed equally

Correspondence: Pengfei Pang, MD, Guangdong Provincial Key Laboratory of Biomedical Imaging and Guangdong Provincial Engineering Research Center of Molecular Imaging, Zhuhai 519000, China.
E-mail: pangpf@mail.sysu.edu.cn
Correspondence: Siyang Wang, MD, The Cancer Center of The Fifth Affiliated Hospital Sun Yat-sen University, Zhuhai 519000, China.
E-mail: 13570608929@163.com
Correspondence: Wuguo Deng, PhD, Sun Yat-sen University Cancer Center, State Key Laboratory of Oncology in South China, Collaborative Innovation Center of Cancer Medicine, Guangzhou 510060, China.
E-mail: dengwg@sysucc.org.cn

that Ku is highly associated with the development of various cancers, including HCC.[13,14] More interestingly, previous reports have revealed that Ku80 deletion is associated with telomere loss and abnormal telomere structure, indicating that Ku80 plays a role in telomere structure maintenance.[15]

In this study, we have identified the XRCC5 protein as a transcriptional regulatory factor that upregulates the expression of hTERT. Mechanistically, the nuclear-factor-erythroid-2-related factor 2 (NRF2) interacts with XRCC5 and regulates hTERT expression and thereby HCC progression. Our clinical data revealed that the expression of XRCC5 and hTERT was positively correlated in HCC tissues and that their elevated expression level was associated with poor prognosis in HCC patients. Collectively, our study throws light on the mechanisms and clinical significance of the XRCC5/NRF2/hTERT signaling axis in HCC progression and will aid in the identification of novel strategies for the diagnosis and treatment of HCC.

RESULTS

XRCC5 binds to the hTERT promoter in HCC cells

To identify the regulator-mediated activity of hTERT promoter in HCC, we used the streptavidin-agarose bead pull-down experiment. In this study, we used a novel 5′-biotin-labeled 362-bp DNA probe targeting the −321 to +41 region of the hTERT promoter (Figure 1A). We incubated this probe with the nuclear proteins extracted from the immortalized liver cell and the four HCC cell lines. Streptavidin-agarose beads were used to pull down the nuclear proteins bound to the 5′-biotin-labeled probe. The proteins were separated on an SDS-PAGE gel. Silver staining showed the dramatic enhancement of a single protein band (between 70 kDa and 100 kDa) in HCC cells compared with L02 cells (Figure 1B). Subsequently, we excised and trypsinized this protein band and analyzed it using MALDI-TOF/TOF mass spectrometry. The results indicated that this protein possessed specific peptides with the sequence VITMFVQR (Figure 1C). Proteomic analysis revealed that the DNA-binding protein, XRCC5, aligned with this sequence (https://blast.ncbi.ncm.nih.gov). Furthermore, owing to its nuclear localization, we hypothesized that XRCC5 might be a promoter-binding protein. We verified this immunofluorescence analysis of Hep3B and SNU449 cells (Figure 1D). Subsequently, we examined several HCC cell lines to identify the nuclear protein expression levels of XRCC5 and hTERT using western blot analysis. As shown in Figure 1E, the nuclear protein levels of XRCC5 and hTERT were higher in the HCC cell lines compared with the L02 cell line.

To further validate whether XRCC5 is a hTERT promoter-binding protein, we pulled down the nuclear protein/DNA complex in different HCC cell lines using the 5′-biotin-labeled hTERT promoter-binding probe or a nonspecific probe (NSP) and detected XRCC5 in the nuclear protein/DNA complex using the XRCC5-specific antibody in western blot analysis. The results showed that XRCC5 specifically bound to the hTERT promoter as a nuclear protein in HCC cells. However, very little amounts of XRCC5 bound to the hTERT promoter-binding probe in L02 (Figure 1F). Furthermore, to confirm the interaction of XRCC5 with the hTERT promoter, we examined its binding to the promoter *in vivo* using chromatin immunoprecipitation (ChIP) assay and found that XRCC5 had a high level of association with the endogenous hTERT promoter in HCC cells (Figure 1G).

XRCC5 protein activates hTERT promoter in HCC cells

To understand whether XRCC5 functions as a transcriptional regulatory factor in the regulation of hTERT promoter activity, we established a dual-luciferase reporter construct containing the hTERT promoter (−321 to +41 bp), which is located upstream of the gene. The luciferase reporter assay demonstrated that XRCC5 knockdown resulted in a remarkable reduction in the promoter activity of hTERT in Hep3B and HepG2 cells, while XRCC5 overexpression significantly increased the hTERT promoter activity in SNU449 and PLC/PRF/5 cells (Figures 2A and 2B). To identify the specific binding region of XRCC5 on the hTERT promoter, eight reporter constructs containing deletions of the hTERT 5′-flanking regions were cloned upstream of the dual-luciferase gene (Figure 2C). As shown in Figures 2D and 2E, there was no significant change in promoter activity when co-transfected with reporter constructs without the region between −144 and −70 bp in XRCC5 knockdown or overexpressing cells, suggesting that the region between −144 and −70 bp on the hTERT promoter was indispensable for XRCC5 binding. These findings indicate that XRCC5 binds to the region between −144 and −70 bp on the hTERT promoter and enhances hTERT promoter activity in HCC cells.

XRCC5 promotes hTERT expression in HCC cell lines

To further explore the role of XRCC5 in modulating hTERT transcription, we established XRCC5 knockdown and overexpression HCC cell lines. As shown in Figures 2F–2I, the inhibition of XRCC5 resulted in a decrease in the mRNA and protein levels of hTERT in Hep3B and HepG2 cells. In contrast, XRCC5 overexpression led to an increase in the mRNA and protein levels of hTERT in SNU449 and PLC/PRF/5 cells. Therefore, we concluded that XRCC5 enhances hTERT expression in HCC cells.

XRCC5 promotes cell proliferation and tumor growth via the hTERT signaling pathway in HCC

To identify the function of XRCC5 in the proliferation of HCC cells, we performed the cell viability and colony formation assays. We found that XRCC5 knockdown inhibited cell viability and colony formation in Hep3B and HepG2 cells compared with a nonspecific short hairpin RNA (shRNA) control (Figures S1A and S1B). In contrast, the overexpression of XRCC5 significantly increased the growth of HCC cells belonging to SNU449 and PLC/PRF/5 cell lines (Figures 3A and 3B). Since XRCC5 modulates hTERT expression, we speculated that XRCC5 promotes the growth of HCC cells through hTERT signaling. To prove this hypothesis, we performed the hTERT overexpression rescue experiment. We found that the inhibition of cell viability and colony formation in Hep3B and HepG2 cells was mediated by XRCC5 knockdown and that this effect could be partly reversed by

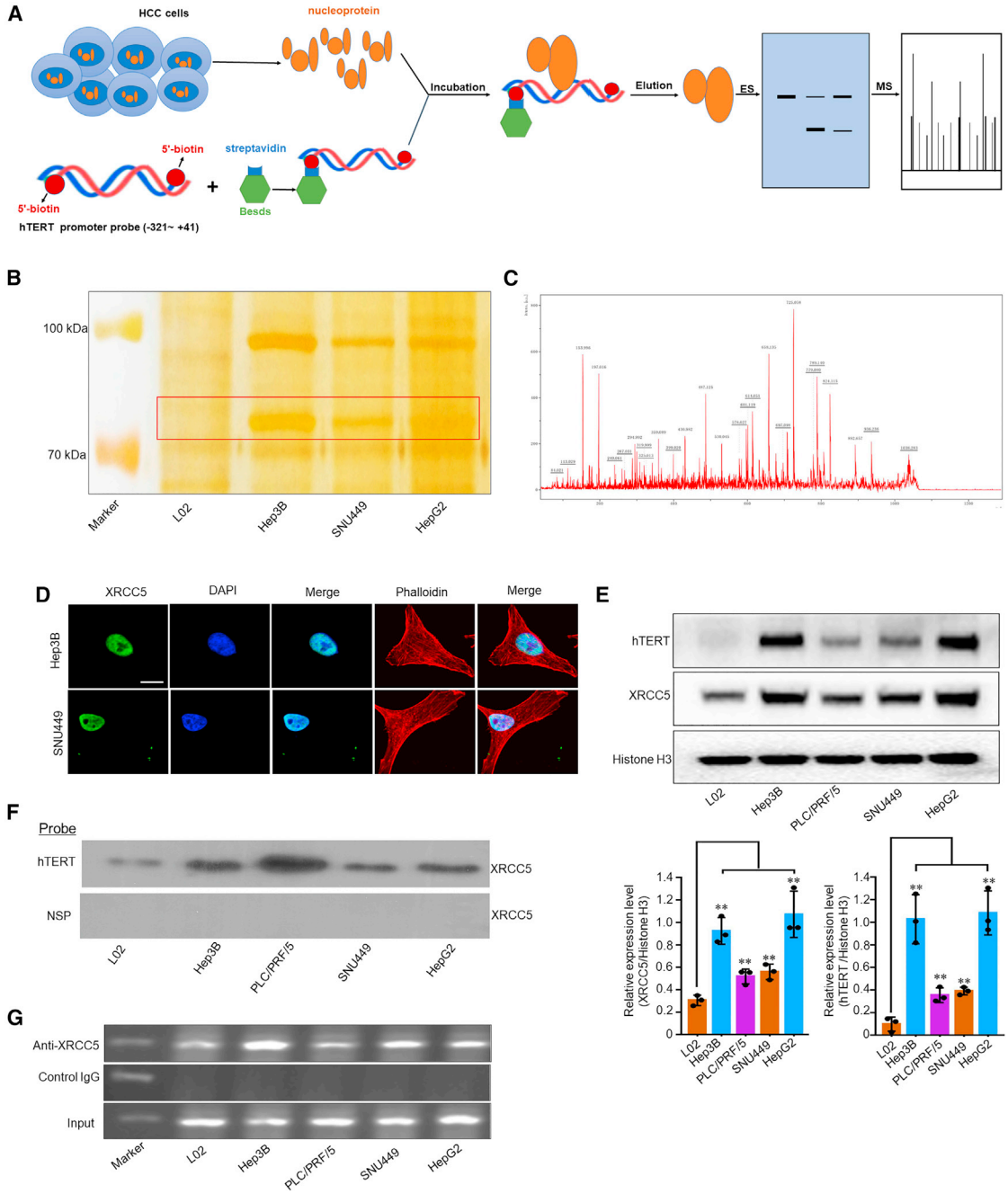

Figure 1. XRCC5 functions as a hTERT promoter-binding protein in HCC cells

(A) Schematic diagram of the streptavidin-agarose pull-down assay with 5′-biotin-labeled 362-bp hTERT promoter-binding probe (−321 to +41 bp). (B) The putative band (red frame) of hTERT promoter-binding proteins pulled down by 5′-biotin-labeled hTERT promoter probes, separated on an SDS-PAGE gel and visualized by silver staining. (C) The marked protein bands were excised, trypsinized, and analyzed by MALDI-TOF/TOF mass spectrometry. (D) Representative immunofluorescent images of XRCC5 expression in Hep3B and SNU449 cells. Green, XRCC5; blue, nucleus; red, cytoskeleton protein. Scale bar, 50 μm. (E) The nuclear protein levels of XRCC5 and hTERT expression in HCC cell lines and immortalized liver cell line (L02) detected by western blot analysis (upper panel). Levels of XRCC5 expression in the HCC cell lines and L02 were quantified relative to Histone H3 (lower panel). Histone H3 was used as the loading control. (F) Detection of the hTERT promoter-bound nuclear proteins in HCC and L02 cells using the streptavidin-agarose bead pull-down assay. A non-specific probe (NSP) was used as the negative control. (G) Chromatin immunoprecipitation (ChIP) assay performed in HCC and L02 cells using anti-XRCC5 antibody. IgG was used as the negative control. Data are presented as mean ± SD of three independent trials, with $^{**}p < 0.01$ determined by Student's t test.

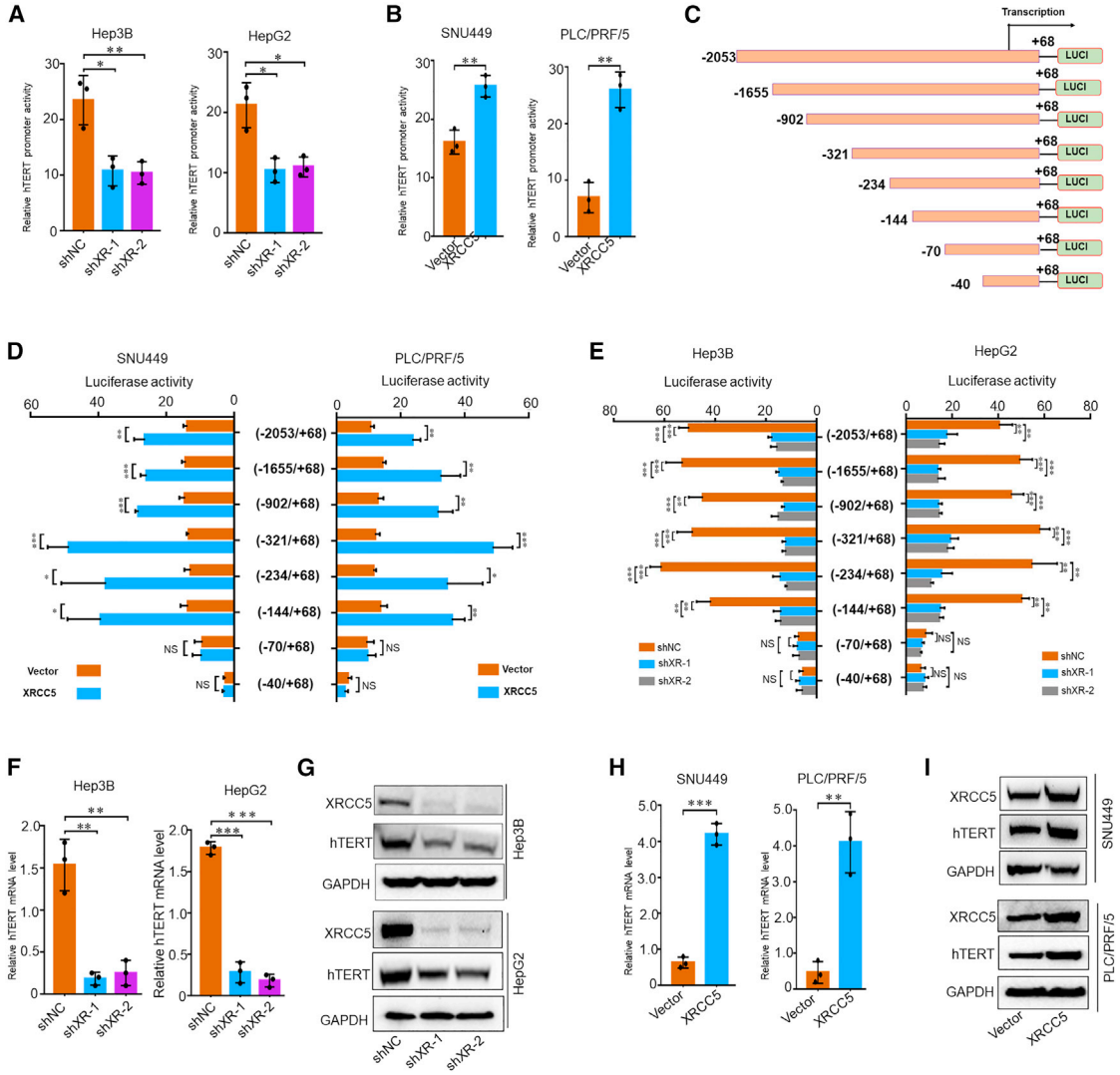

Figure 2. XRCC5 activates the promoter and expression of hTERT in HCC cell lines

(A and B) Relative hTERT promoter activity in XRCC5 knocked down Hep3B and HepG2 cells (A). Relative hTERT promoter activity in XRCC5 overexpressing SNU449 and PCL cells (B). Relative hTERT promoter activity was determined by dual-luciferase assay. (C) Construction of hTERT promoter-based reporters by 5′ sequential deletion. (D and E) Serially truncated hTERT promoter constructs co-transfected with XRCC5 or vector (D) or shNC or shXRCC5 (E) and their relative luciferase activity. (F–I) Expression of hTERT mRNA, measured by qPCR, in XRCC5 knocked down Hep3B and HepG2 cells (F). hTERT protein expression, measured by western blot analysis, in XRCC5 knocked down Hep3B and HepG2 cells (G). Expression of hTERT mRNA, measured by qPCR, in XRCC5-overexpressing SNU449 and PLC/PRF/5 cells (H). hTERT protein expression, measured by western blot analysis, in XRCC5-overexpressing SNU449 and PLC/PRF/5 cells (I). Data are presented as mean ± SD of three independent trials, with *p < 0.05, **p < 0.01, and ***p < 0.001 determined by Student's t test.

hTERT overexpression (Figures 3C and 3D). To further demonstrate that XRCC5 promotes tumor growth via the hTERT signaling pathway *in vivo*, we established an HCC xenograft model in nude mice. BALB/c nude mice aged 4–6 weeks were randomly divided into four groups. The flank of the nude mouse was inoculated with Hep3B cells showing stable expression of XRCC5-shRNAs or control shRNAs or groups of XRCC5 knockdown with or without hTERT overexpression. Following monitoring of the tumor growth for 21 days, the tumors were excised from each mouse and the tumor size and weight were determined. We found that the size and weight of HCC tumors in the XRCC5 knockdown group were significantly reduced compared with the control shRNA group (Figures 3E, S1C, and S1D). However, xenograft tumors in the group with XRCC5 knockdown and hTERT overexpression grew faster, both in size and weight, compared with the group with XRCC5 knockdown alone (Figures 3E, S1C, and S1D). These findings indicate that XRCC5 promotes the proliferation of HCC cells via the hTERT signaling pathway.

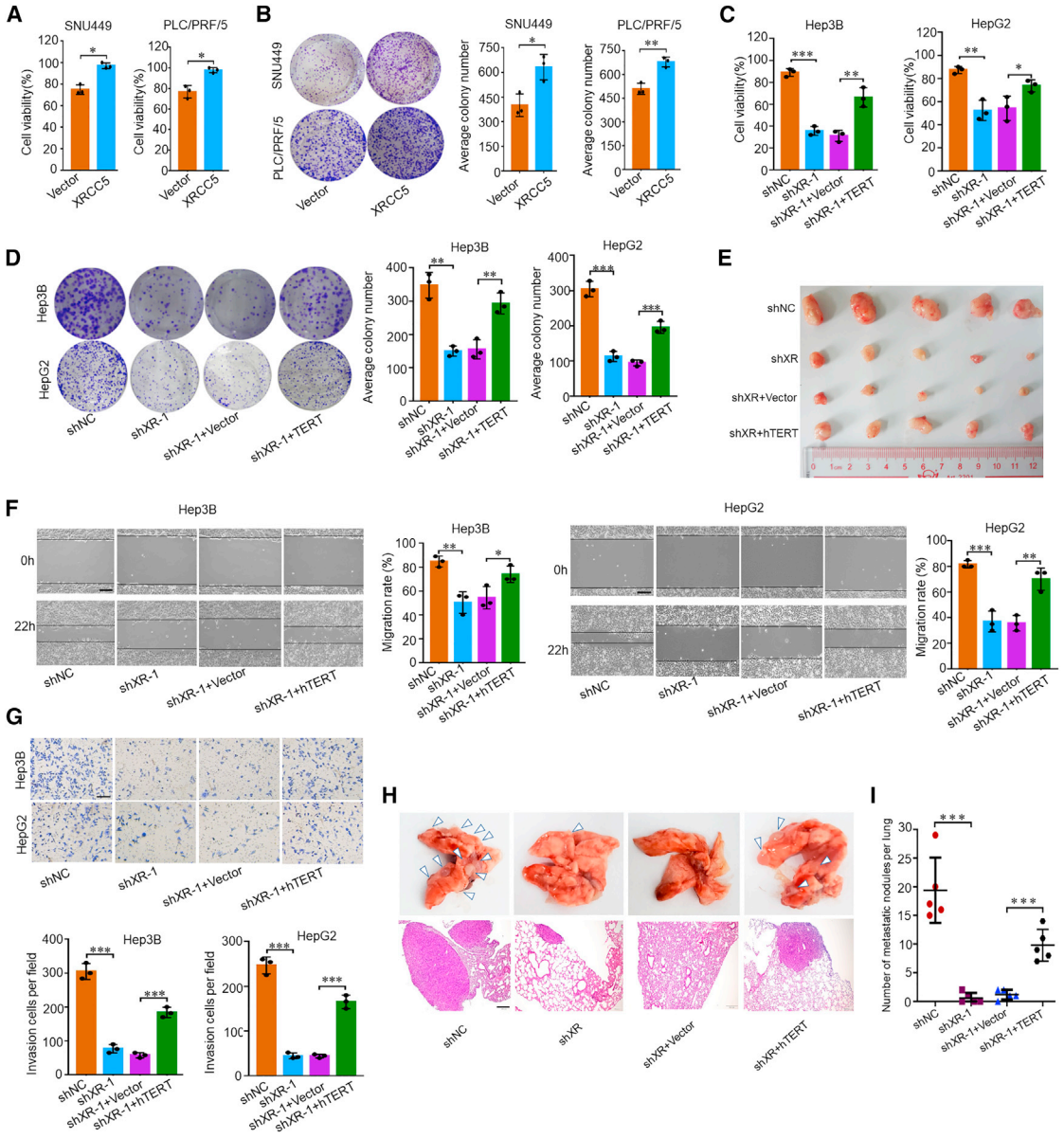

Figure 3. XRCC5 promotes tumor growth and metastasis via the hTERT signaling pathway in HCC

(A and B) Human SNU449 and PLC/PRF/5 cells transfected with an XRCC5-overexpressing vector or an empty vector. Cell viability (A) and colony formation (B) are analyzed by the CCK8 and colony formation assays, respectively. (C and D) Hep3B and HepG2 cells transfected with control shRNA (shNC), XRCC5 shRNA (shXR), XRCC5 shRNA + control vector (shXR + vector), and XRCC5 shRNA + hTERT overexpression plasmid (shXR + hTERT), respectively. Cell viability (C) and colony formation (D) are analyzed by the CCK8 and colony formation assays, respectively. (E) Representative images of tumors derived from BALB/c nude mice subcutaneously injected with shNC, XRCC5-shRNA, XRCC5 knockdown and hTERT overexpression, or XRCC5 knockdown and control vector Hep3B cells. (F and G) Hep3B and HepG2 cells transfected with shNC, shXR, shXR + vector, and shXR + hTERT, respectively. Cell migration (F) and invasion (G) are analyzed by the wound healing and trans-well assays, respectively. Scale bars, 200 μm. (H) Representative images (upper panel) and HE staining (lower panel) of the lung tissues from nude mice treated with shNC, XRCC5-shRNA, XRCC5 knockdown and hTERT overexpression, or XRCC5 knockdown and control vector Hep3B cells. Arrowheads showed the representative results of metastatic lung nodules. Scale bar, 100 μm. (I) The amount of metastasis tumor nodules was calculated. Data are presented as mean ± SD of three independent trials, with *$p < 0.05$, **$p < 0.01$, and ***$p < 0.001$ determined by Student's t test.

XRCC5 promotes cell migration, invasion, and tumor metastasis via the hTERT signaling pathway in HCC

Metastasis is a significant determinant of the prognosis and overall survival time of HCC patients. Therefore, we investigated the role of XRCC5 in the migration and invasion of HCC cells. As shown in Figures S1E and S1F, XRCC5 overexpression promoted the migration and invasion of SNU449 and PLC/PRF/5 cells compared with the control vector. Similarly, XRCC5 knockdown suppressed the

migration and invasion of Hep3B and HepG2 cells (Figures 3F and 3G). Moreover, the suppression of the migration and invasion of Hep3B and HepG2 cells by XRCC5 knockdown could partly be reversed by hTERT overexpression (Figures 3F and 3G). Moreover, in the lung metastatic model, we found that stable knockdown of XRCC5 significantly reduced the number of lung metastatic nodules (Figures 3H and 3I). However, the group with XRCC5 knockdown and hTERT overexpression rescued the number of lung metastatic nodules compared with the group with XRCC5 knockdown alone (Figures 3H and 3I). Collectively, we proved that XRCC5 enhances the cell migration, invasion, and tumor metastasis via the hTERT signaling pathway in HCC.

XRCC5 regulates the chemosensitivity of HCC cells to 5-Fu via hTERT signaling

Clinically, 5-fluorouracil (5-Fu) is a chemotherapeutic drug that is commonly used for HCC patients. However, resistance to 5-Fu is becoming a major problem, since it affects its efficiency in HCC treatment. Since a previous report demonstrated that 5-Fu could promote the anti-telomerase activity of HCC cells,[16] we hypothesized that the XRCC5-mediated regulation of hTERT expression might be responsible for the sensitivity of HCC cells to 5-Fu. To test this hypothesis, HCC cells in which XRCC5 was knocked down or overexpressed were exposed to a medium containing various concentrations of 5-Fu for 48 h. As shown in Figures 4A and 4B, XRCC5 or hTERT overexpression increased the resistance to 5-Fu in SNU449 and PLC/PRF/5 cells, while XRCC5 knockdown increased the sensitivity to 5-Fu in Hep3B and HepG2 cells. The half-maximal inhibitory concentration (IC50) values of 5-Fu in SNU449 and PLC/PRF/5 cells overexpressing XRCC5 or hTERT were higher compared with the corresponding control cells (Figure S2A), while the IC50 values of 5-Fu in HCC cells in which XRCC5 was knocked down were lower compared with the corresponding control cells (Figure S2B). Moreover, the inhibition of colony formation, migration, and invasion caused by 5-Fu could be reversed by hTERT overexpression (Figures 4C–4E and S2C). Furthermore, we explored whether XRCC5 regulates the chemosensitivity of HCC cells to 5-Fu *in vivo* via the hTERT signaling pathway. We found that the size and weight of xenograft (Figures 4E, S2D, and S2E), as well as the number of lung metastatic nodules (Figures 5F and S2F), in the control shRNA group receiving 5-Fu treatment were reduced in contrast to the shRNA group receiving PBS. In addition, a prominent reduction was seen in the tumor size and weight, as well as the number of lung metastatic nodules, of the XRCC5-shRNA group receiving 5-Fu treatment, and the efficiency of 5-Fu could be partly reversed by hTERT overexpression (Figures 4E, 4F, and S2D–S2F). Collectively, these findings suggest that XRCC5 modulates the chemosensitivity of HCC cells to 5-Fu through the hTERT signaling pathway *in vitro* and *in vivo*.

XRCC5 regulates hTERT expression and HCC progression in a NRF2-dependent manner

NRF2 is a transcription factor that plays an important role in the development of various human tumors, including HCC.[17] Previous reports reveal that NRF2 is a transcription factor of hTERT.[18] Our result also showed that NRF2 was a hTERT promoter-binding protein (Figure 5A). We hypothesized that XRCC5 functions synergistically with NRF2 and modulates hTERT expression and HCC progression. To verify this hypothesis, we performed the immunofluorescence assay and studied NRF2 localization, since subcellular distribution frequently determines protein function. We found that NRF2 was located in the nucleus, co-localized with XRCC5 (Figure 5B). The expression level of NRF2 was positively correlated with XRCC5 in HCC cell lines (Figure S3A). Further, co-immunoprecipitation assay showed that XRCC5 interacted with NRF2 (Figures 5C and 5D). As shown in Figure S3B, the inhibition of NRF2 resulted in a decrease in the protein levels of hTERT in Hep3B and HepG2 cells. However, the expression of XRCC5 did not change significantly with NRF2 knockdown. Functionally, NRF2 knockdown inhibited cell viability, colony formation, migration, and invasion in Hep3B and HepG2 cells (Figures S3C–S3F). In addition, we found that XRCC5-mediated hTERT upregulation was insignificant when NRF2 was knocked down, suggesting that XRCC5-regulated hTERT expression is NRF2 dependent (Figure 5E). We also demonstrated that the promotion of cell viability, colony formation, migration, and invasion of HCC cells by XRCC5 via hTERT signaling was NRF2 dependent (Figures 5F–5I). These findings suggest that XRCC5 regulates hTERT expression and HCC progression in a NRF2-dependent manner.

High level of XRCC5 and hTERT expression is associated with poor clinical outcome in HCC patients

To further explore the association between XRCC5 and hTERT in HCC patients, we used two individual cohorts (cohort 1 [n = 94] and cohort 2 [n = 90]) of HCC tissues with corresponding non-tumor tissues to determine the expression levels of XRCC5 and hTERT (Table S1). Both XRCC5 and hTERT levels were significantly increased in HCC tissues compared with that in non-tumor tissues (Figures 6A, 6B, and S4A). Moreover, analysis of The Cancer Genome Atlas (TCGA) database also found that both XRCC5 and hTERT were frequently upregulated in HCC tissues (Figures S4B and S4C). Correlation analysis revealed that the expression of XRCC5 was positively associated with that of hTERT (Figure 6C). Multivariate analysis indicated that Edmondson grade, tumor size, and XRCC5 level were independent prognostic factors for the overall survival (OS) of HCC patients (Table 1). Furthermore, we explored the association between XRCC5 level and different clinicopathological variables in HCC patients in two cohorts. High expression level of XRCC5 was associated with Edmonson grade, American Joint Committee on Cancer (AJCC) grade, T stage, and tumor size (Tables S2–S4). In addition, we investigated the potential role of XRCC5 and hTERT on the prognosis of HCC. Based on the median value of XRCC5 or hTERT expression levels, 184 HCC patients were divided into two groups. Patients with high expression levels of XRCC5 and/or hTERT showed remarkably lower overall survival times compared with those with low expression levels of XRCC5 and/or hTERT (Figures 6D–6F and S4D–S4G). In conclusion, the XRCC5 expression is positively correlated with that of hTERT and the synergistic expression of both XRCC5 and hTERT is strongly associated with the poor prognosis of HCC.

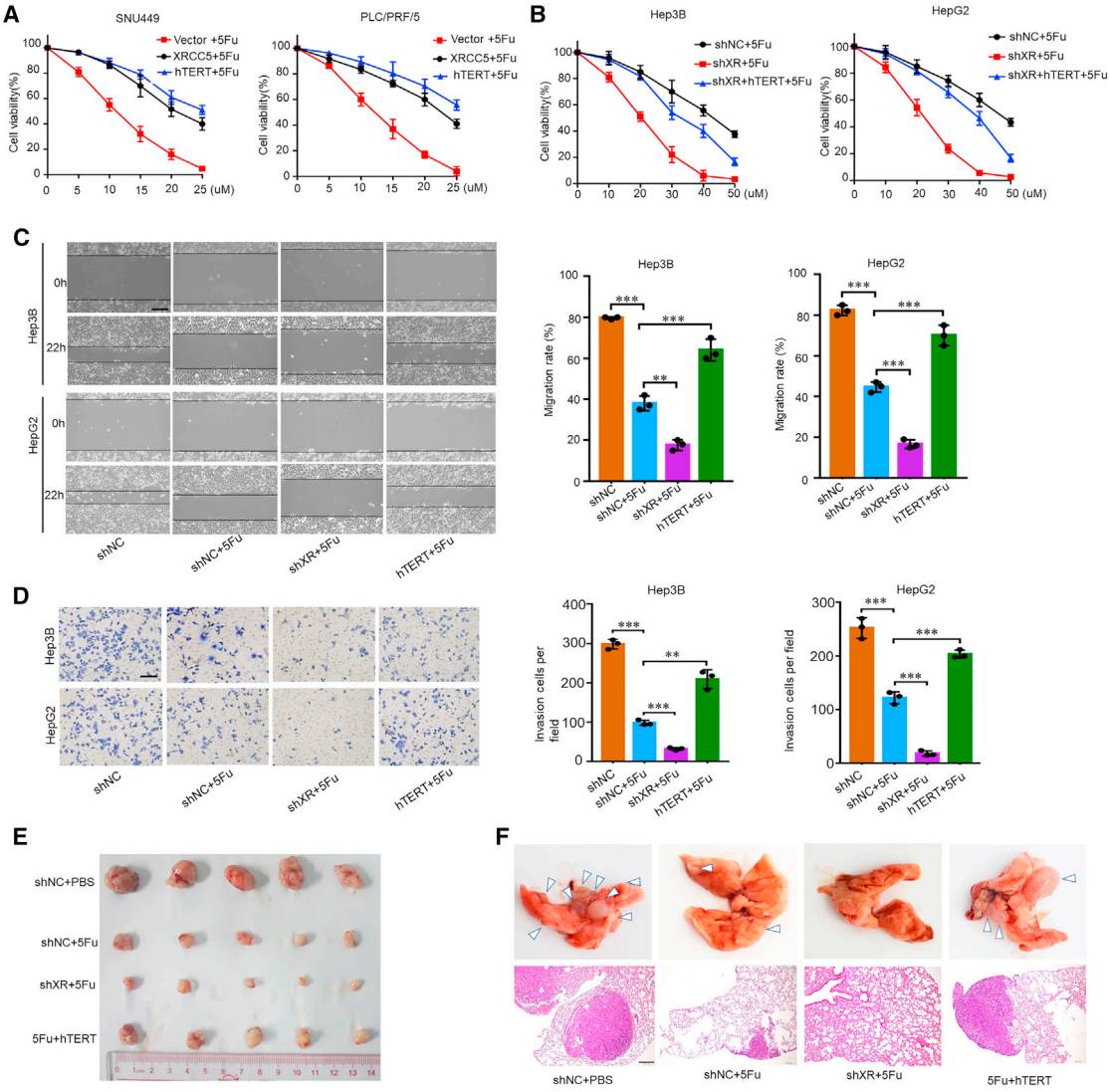

Figure 4. XRCC5 regulates the chemosensitivity of HCC cells to 5-Fu via the hTERT signaling pathway

(A) Cell viability, determined by the CCK8 assay, in XRCC5-overexpressing, hTERT-overexpressing, or control vector containing SNU449 and PLC/PRF/5 cells treated with 5-Fu. (B) Exposure of Hep3B and HepG2 cells transfected with shNC, shXR, or shXR + hTERT to 5-Fu. Cell viability was determined by the CCK8 assay. (C and D) Exposure of Hep3B and HepG2 cells transfected with shNC, shXR, or hTERT-overexpressing plasmid to 5-Fu. Cell migration (C) and invasion (D) were detected by the wound healing and trans-well assays, respectively. Scale bars, 200 μm. (E) Representative images of tumors at 21 days post-subcutaneous injection of Hep3B cells with XRCC5-shRNA, control shRNA, or hTERT overexpression and intraperitoneal injection of 5-Fu into BALB/c nude mice every 2 days. (F) Representative images (upper panel) and HE staining (lower panel) of the lung tissues from nude mice treated with Hep3B cells with XRCC5-shRNA, control shRNA, or hTERT overexpression and intraperitoneal injection with 5-Fu. Arrowheads showed the representative results of metastatic lung nodules. Scale bar, 100 μm. Data are presented as mean ± SD of three independent trials, with *$p < 0.05$, **$p < 0.01$, and ***$p < 0.001$ determined by Student's t test.

DISCUSSION

In the current study, XRCC5 was identified as a transcriptional regulatory factor binding to the hTERT promoter and activating the transcription of hTERT. Furthermore, XRCC5 regulated hTERT expression in a NRF2-dependent manner (Figure 6G). XRCC5 was found to be overexpressed in HCC tissues, relative to the corresponding, adjacent non-tumor tissues in two cohorts. The expression of XRCC5 was closely associated with the size and Barcelona Clinic Liver Cancer (BCLC) stage of the tumor. XRCC5 expression also showed strong correlation with HCC formation and progression. Thus, our results indicate that XRCC5 functions as an oncogene in HCC and that it can be considered as a potential prognostic indicator of HCC.

hTERT is overexpressed in 80%–95% of cancers, including HCC. It plays a pivotal role in cell immortalization and malignant

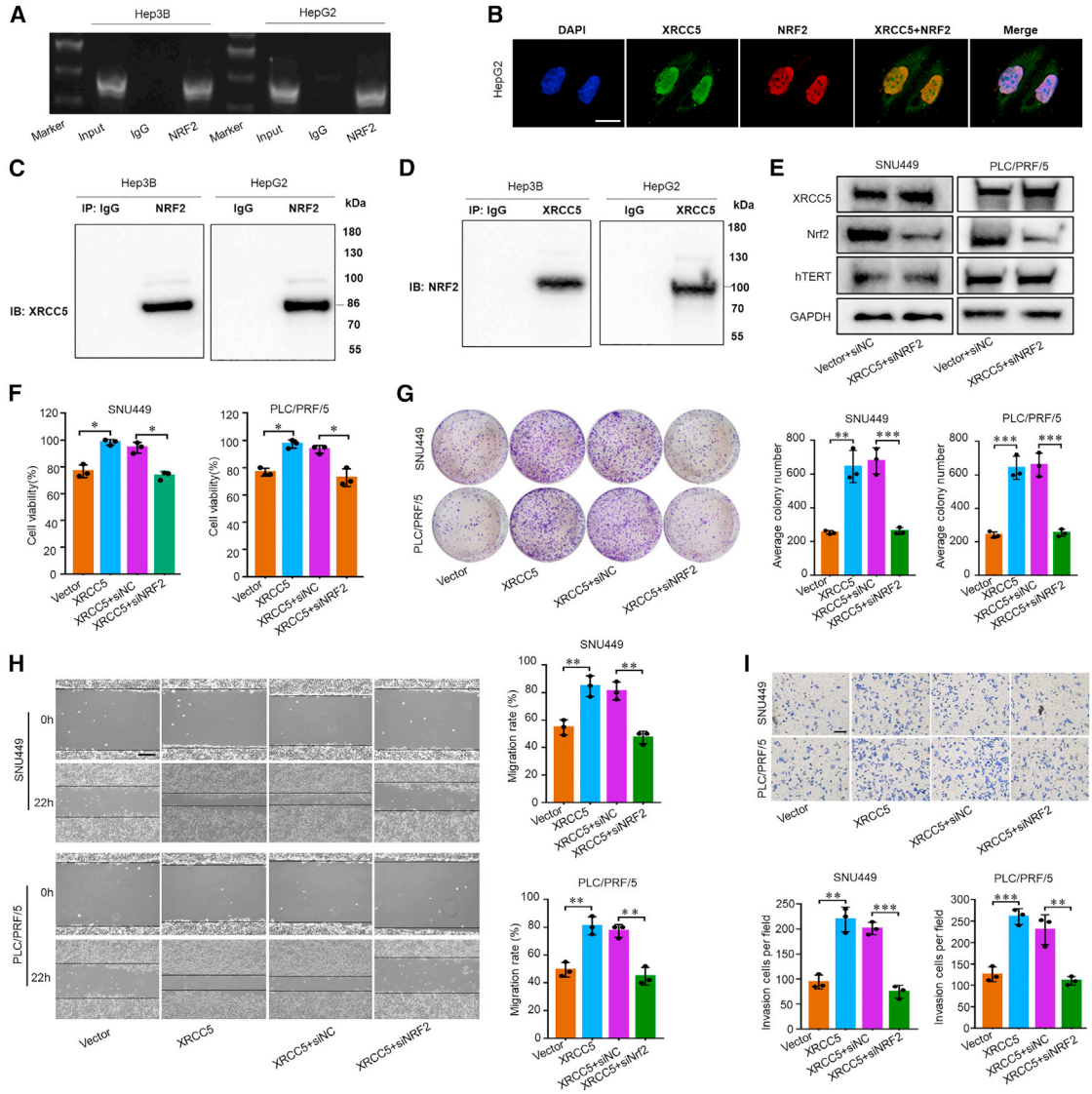

Figure 5. XRCC5 regulates hTERT expression and HCC progression in a NRF2-dependent manner

(A) Chromatin immunoprecipitation (ChIP) assay performed in HepG2 cells using anti-NRF2 antibody. IgG was used as the negative control. (B) Representative immunofluorescent images of XRCC5 and NRF2 expression in Hep3B and HepG2 cells. Green, XRCC5; red, NRF2; blue, nucleus. Scale bar, 50 μm. (C and D) Immunoprecipitation of the extracted Hep3B and HepG2 cell proteins with anti-NRF2 antibody (C) or anti-XRCC5 antibody (D). The precipitates were analyzed by western blot. (E) The expression of hTERT protein, measured by western blot analysis, in control vector and NRF2-siNC or XRCC5 overexpression and NRF2-siRNA Hep3B cells. GAPDH was used as the loading control. (F and G) Cell viability and (F) colony formation (G) measured in SNU449 and PLC/PRF/5 cells with XRCC5 overexpression, XRCC5 overexpression and NRF2-siRNA, or XRCC5 overexpression and control siRNA. (H and I) Cell migration (H) and invasion (I) detected in SNU449 and PLC/PRF/5 cells with XRCC5 overexpression, XRCC5 overexpression and NRF2-siRNA, or XRCC5 overexpression and control vector. Scale bars, 200 μm. Data are presented as mean ± SD of three independent trials, with *p < 0.05, **p < 0.01, and ***p < 0.001 determined by Student's t test.

transformation.[19] However, the underlying molecular mechanisms of the re-activation of hTERT during tumorigenesis is not fully understood. Previous studies have indicated that hTERT gene amplification and mutation are responsible for its overexpression in tumors.[20,21] We previously reported that RBFOX3, a hTERT promoter-binding protein, transcriptionally upregulated hTERT expression in HCC cells.[22] Here, we demonstrated for the first time that the high expression level of the XRCC5 protein was another factor responsible for the upregulation of hTERT expression in HCC cells.

XRCC5, also known as Ku80, is best known for its function in DNA damage repair. It forms a heterodimer with Ku70 and facilitates homologous recombination (HR) and non-homologous end joining (NHEJ).[12,23] However, increasing evidence has shown that XRCC5

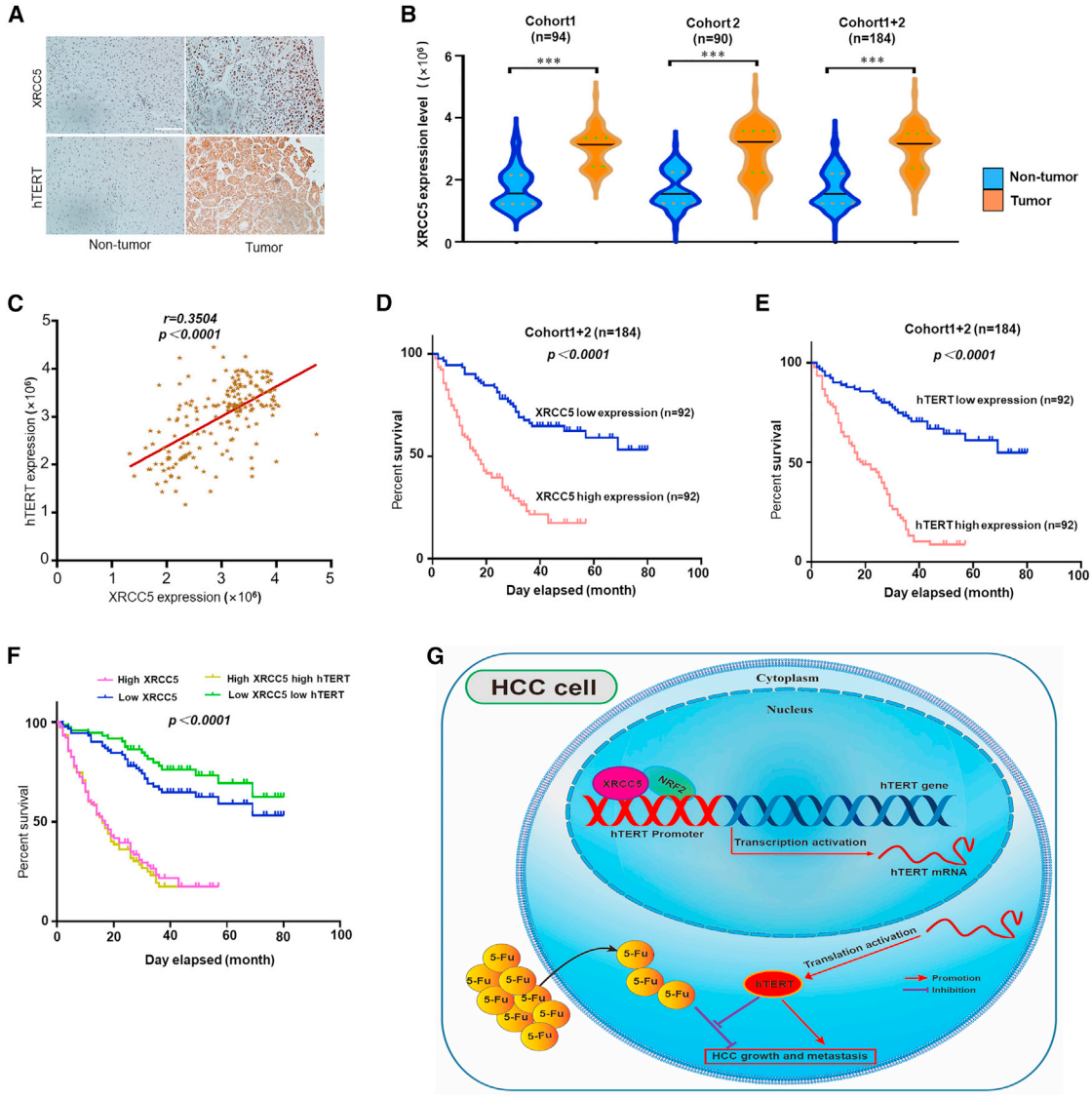

Figure 6. High expression level of XRCC5 and hTERT is associated with poor clinical outcomes in HCC patients

(A) Representative images of the immunohistochemical staining of XRCC5 and hTERT proteins in HCC tumor or non-tumor tissues. Scale bar, 200 μm. (B) Immunohistochemistry assay for the expression of XRCC5 in HCC tumor or non-tumor tissues from 184 patients. (C) Pearson correlation analysis between XRCC5 and hTERT expression in 184 HCC tissue samples. (D and E) Kaplan-Meier overall survival curves for HCC patients with high (red line) or low (blue line) expression level of XRCC5 (D) or hTERT (E) from cohort 1 + 2. (F) Kaplan-Meier overall survival curves for HCC patients with high (red line) or low (blue line) expression level of XRCC5 and high (yellow line) or low (green line) expression level of both XRCC5 and hTERT. (G) The schematic diagram illustrating molecular mechanisms by which XRCC5 drove tumor progression and 5-Fu insensitivity in hepatocellular carcinoma. ***p < 0.001 determined by Student's t test.

participates in cellular processes associated with cancer development.[24–30] Apart from its role in DNA damage repair, XRCC5 has been reported to function as a transcriptional regulatory factor. For example, XRCC5 binds to the promoter of grp94,[31] apolipoprotein C-IV,[32] S100A9,[33] and interleukin-2 (IL-2)[34] and regulates their genetic transcription. With respect to cancer, Mayeur et al. reported the involvement of XRCC5 in the transcriptional recycling coactivator of the androgen receptor in prostate cancer cells.[35] Our previous studies showed that XRCC5 regulates the transcription of COX-2 and PDK-1 in lung cancer and melanoma, respectively.[36,37] In this study, we identified that XRCC5 functions as a hTERT promoter-binding protein.

With regards to the mechanisms underlying the regulation of hTERT expression in lung cancer, we have demonstrated for the first time that hTERT is transcriptionally activated by XRCC5 in a NRF2-dependent manner. NRF2 is a transcription factor that is activated by cell stress.[38] Upon activation, NRF2 accumulates in the nucleus and binds to its consensus sequence in the promoter

Table 1. Univariate and multivariate analyses of OS in 184 HCC patients by Cox regression analysis

		Univariate analysis			Multivariate analysis		
Variables		HR	95% CI	p value	HR	95% CI	p value
Gender	male versus female			0.397			NS
Age (years)	> 55 versus ≤55			0.352			NS
Edmondson grade	I + II versus III + IV	0.797	0.640–0.993	0.043	0.799	0.643–0.992	0.042[a]
AJCC grade	1 + 2 versus 3 + 4			0.055			NS
Tumor size (cm)	> 3 versus ≤3	0.623	0.423–0.918	0.017[a]	0.625	0.425–0.919	0.017[a]
XRCC5	high versus low	3.737	2.451–5.698	< 0.001[a]	2.485	1.549–3.987	< 0.001[a]

CI, confidence interval; HR, hazard ratio; NS, not significant.
[a]$p < 0.05$ was considered statistically significant

of the target genes, thereby inducing their transcription. Increasing evidence suggests that NRF2 plays an important role in the promotion of tumorigenesis in certain models.[39] Recently, NRF2 has been described as an oncogene in HCC, and it plays an important role in cell proliferation and tumorigenesis.[40–43] In this study, we demonstrated that NRF2 interacts with XRCC5 and then binds to the hTERT promoter to activate the transcription of hTERT.

MATERIALS AND METHODS

Cell lines and cell culture

The Hep3B, HepG2, PLC/PRF/5, and SNU449 cell lines were obtained from the American Type Culture Collection (ATCC) (Manassas, VA, USA), while the L02 cell line was obtained from the Chinese Academy of Sciences Cell Bank (Shanghai, China). The cells were authenticated by short tandem repeat (STR) profiling and were confirmed to be mycoplasma free before use. All cell lines were cultured in DMEM supplemented with 10% fetal bovine serum (FBS) and antibiotics in a humidified atmosphere with 5% CO_2 at 37°C.

Drugs and antibodies

5-Fu (99.9% purity) was purchased from Selleck Chemicals (Houston, TX), dissolved in DMSO (20 mol/L), and stored at −20°C. The stock was diluted with culture medium before use. Immunoglobulin G (IgG) (no. 2729) and antibodies for XRCC5 (no. 2753), NRF2 (no. 12721), and GAPDH (no. 5174) were purchased from Cell Signaling Technology (Danvers, MA), while the hTERT antibody was purchased from Novus Biologicals (NB100-317).

Streptavidin-agarose pull-down assay

Briefly, a biotin-labeled, double-stranded DNA probe corresponding to the nucleotides in the region −875 to +40 bp of the hTERT promoter was synthesized by PCR with a pair of biotin-labeled primers (forward: 5′-GCCCTCGCTGGCGTCCCTGC-3′; reverse: 5′-GGCC GGGGCCAGGGCTTCCCACG-3′). Nuclear proteins were extracted from the cell lines. Approximately 8 μg of the hTERT promoter probe was mixed with 800 μg of nuclear proteins and 80 μL of streptavidin-agarose beads, with constant rotation, at 4°C overnight. Subsequently, the beads were collected by low-speed centrifugation and washed three times with lysis buffer. The samples were then eluted with SDS loading buffer by boiling at 100°C for 5–10 min. The pulled-down proteins were separated by polyacrylamide gel electrophoresis and visualized by silver staining.

ChIP assay

For ChIP assay, about 10^7 cells of each sample were cross-linked using 1% formaldehyde for 10 min at room temperature with slow shaking. Subsequently, the cross-links were quenched by adding 1.375 M glycine. Following centrifugation at 1,000 rpm for 5 min, the sediment was collected and lysed with ChIP lysis buffer on ice for 30 min. Following centrifugation at 14,000 rpm in a cold room for 15 min, the supernatant was removed. The sediment was re-suspended in lysis buffer and sonicated for 10 min and centrifuged at maximum speed in a cold room for 10 min. Following centrifugation, the supernatant was collected. Antibody and sheared salmon sperm DNA were added to the supernatant and incubated overnight in a cold room with rotation. The mixture was then washed thrice with wash buffer and twice with TE buffer. To reverse the cross-links, the beads were re-suspended in ChIP elusion buffer supplemented with 1 μL proteinase K and incubated overnight at 65°C. Subsequently, DNA purification was performed using a DNA purification kit (TAKARA) and the purified DNA was used as template in a PCR.

Transient transfection

The Hep3B and HepG2 cells were cultured and transfected with NRF2-specific small interfering RNA (siRNA) (siNRF2) (5′-UAAUU-GUCAACUACUGUCAGUU-3′) or negative control (siNC) using Lipofectamine 3000 (Invitrogen, USA), according to manufacturer's instructions. The treated and control cells were grown in an incubator for 48 h and collected subsequently for experimental use.

Lentiviral construction and cell transfection

Stable expression cells were constructed using the lentiviral system. XRCC5 was knocked down in Hep3B and HepG2 cells using a XRCC5 lentiviral construct expressing XRCC5-targeted shRNA (shXR1, 5′-CTAAAGTGGATGAGGAACA-3′ and shXR2, 5′-GCAA AGAAGGTGATAACCA-3′; Genechem, Shanghai, China). Cells with reduced expression of XRCC5 were selected with puromycin (1.0 μg/mL) for 7–14 days following lentiviral infection. Cells overexpressing XRCC5 were constructed using a lentivirus overexpressing XRCC5, following the aforementioned procedure.

Promoter reporters and dual-luciferase assay

The hTERT promoter was cloned into the pGL3-basic vector to construct the luciferase reporter plasmid. To detect the relative luciferase activity, the HCC cells were seeded in 96-well plates, at a density of 3.0×10^3 cells/well, and transfected with promoter-luciferase plasmid and pRL-CMV (Renilla luciferase). The luciferase activity was measured using a dual-luciferase assay kit (Promega, Madison, WI) at 48 h post-transfection.

Cell viability assay

HCC cells were seeded in 96-well plates, and the cell viability was assessed using a cell counting kit-8 (CCK-8) (KeyGEN BioTECH, Jiangsu, China). Following 72 h of growth, the absorbance was measured at 450 nm using a microplate reader.

Colony formation assay

Approximately 500 cells were seeded in 6-well plates and cultured for 14 days. Subsequently, the colonies were stained with 1% crystal violet and the number of colonies were counted.

Wound healing and trans-well invasion assays

In HCC cells that grew naturally to full confluency in 6-well plates, a vertical wound was inflicted using a 200 μL sterile pipette tip. The wounded cells were incubated for 6 h in DMEM without FBS. Following incubation, they were washed with PBS to remove the detached cells. Subsequently, the cells were treated with different reagents. They were incubated in DMEM without FBS for another 24 or 48 h, and the wound gap was measured. The cells were photographed using an inverted microscope. Subsequently, the trans-well invasion assay was performed to test the invasion of cells. Briefly, the inner side of the bottom of the upper chamber (BD Biosciences) was coated with 1 mg/mL Matrigel Matrix (Becton Dickinson, Franklin Lakes, NJ) such that each well contained 20 μL, and the wells were air dried naturally. The lower chamber contained 500 μL DMEM with 20% FBS. About 3×10^5 cells in 100 μL DMEM without FBS were added to the upper chamber, which was placed in a 24-well plate and incubated at 37°C with 5% CO_2 for 22 h. The cells in the underside of the filter were fixed using 4% paraformaldehyde for 15 min. Subsequently, the cells were stained with crystal violet for 15 min. Cell images were obtained using an inverted microscope at 50× magnification.

Western blot

Cells were lysed using lysis buffer on ice for 30 min. Subsequently, they were centrifuged at 14,000 rpm at 4°C. The proteins in the supernatant were collected and boiled with SDS loading buffer at 100°C for 8 min. The protein concentration was measured using a bicinchoninic acid (BCA) kit. SDS-PAGE and western blot analysis were performed according to standard procedures.

RT-PCR and real-time PCR (qPCR)

Total RNA was extracted using the RaPure Total RNA Micro Kit (Magen, Guangzhou, China). First-strand cDNA was synthesized using HiScript II One Step RT-PCR Kit (Vazyme, Nanjing, China), according to the manufacturer's instructions. qPCR was performed using ChamQ SYBR qPCR Master Mix (Vazyme, Nanjing, China) following the manufacturer's instructions.

Co-immunoprecipitation assays (coIP)

For coIP, about 1.0×10^7 cells were collected and lysed with IP lysis buffer on ice for 30 min. Following centrifugation at 14,000 rpm at 4°C for 10 min, the supernatant was collected and incubated with specific antibody overnight at 4°C with rotation. Subsequently, protein A/G agarose was added and the mixture was incubated at 4°C with rotation for 2 h. The beads were spun down at 2,500 rpm for 1 min, and the supernatant was removed. The beads were washed thrice with washing buffer A for 5 min, once with washing buffer B, and twice with washing buffer C. Subsequently, the beads were spun down at 2,500 rpm for 1 min and the supernatant was removed. The beads were then eluted in SDS sample loading buffer and boiled for 5 min. Finally, the proteins were separated by SDS-PAGE.

Confocal immunofluorescence

Briefly, cells were fixed with 4% paraformaldehyde for 15 min, permeabilized with 0.5% Triton X- for 5 min, and blocked with 5% BSA for 30 min. Subsequently, primary antibodies were incubated with the cells at 4°C overnight, with 1% BSA in PBS as the negative control. Later, secondary antibodies were added to the samples and incubated at room temperature for 30 min. The cell nuclei were stained with 0.5 μg/mL of 4′,6-diamidino-2-henylindole (DAPI) and visualized under a microscope.

Immunohistochemistry (IHC) staining

HCC tissues were fixed in 10% neutral-buffered formalin overnight and dehydrated using increasing concentration gradients. Paraffin-embedded tumor tissues were processed for immunohistochemical staining with XRCC5 and hTERT antibodies and incubated overnight at 4°C in a humidified chamber. Subsequently, they were washed thrice with PBS and treated with a non-biotin horseradish peroxidase detection system, according to manufacturer's instructions (Dako). IHC scores were calculated using the Image-Pro Plus 6 software, according to the manufacturer's instructions.

Animal study

Animal experiment protocols were approved by the Animal Care Committee of Sun Yat-sen University Cancer Center. All animal procedures were performed in accordance with the Guide for the Care and Use of Laboratory Animals (NIH publications nos. 80-23, revised 1996) and the Institutional Ethical Guidelines for Animal Experiments developed by Sun Yat-sen University. BALB/c female nude mice (Vital River Laboratory Animal Technology, Beijing, China) aged 4–6 weeks were injected with Hep3B cells, control shRNA, XRCC5 shRNA, vector, or hTERT overexpression plasmid. Five animals were used for each group. Following tumor development, the length (L), width (W), and height (H) of each tumor was measured using calipers. At the end of the experiment, the mice were humanely sacrificed and tumors and lungs were harvested. The volume (V) was calculated as follows: $V\ (mm^3) = \pi/6 \times L \times W^2$.

SUPPLEMENTAL INFORMATION

Supplemental information can be found online at https://doi.org/10.1016/j.omto.2021.12.012.

ACKNOWLEDGMENTS

This work was supported by funds from the National Natural Science Foundation of China, China (81802936 and 81972569); the Guangdong Basic and Applied Basic Research Foundation (2020A 1515010016); and the Science and Technology Project Foundation of Zhuhai, China (20181117A010005). This work was done with the approval of the Medical Ethics Committee of The Fifth Affiliated Hospital of Sun Yat-sen University. The mice used in this study were cared for and handled according to animal protocols approved by the Animal Care Committee of The Fifth Affiliated Hospital of Sun Yat-sen University.

AUTHOR CONTRIBUTIONS

This work was carried out in collaboration between all authors. T.L., S.W., P.P., and W.D. defined the research theme and designed the experimental approach. T.L., Q.L., H.G., L.L., H.L., X.H., and L.Y. carried out the experiments. T.L., Q.L., H.G., L.L., and W.D. analyzed the data and interpreted the results. T.L., Q.L., H.G., L.L., X.H., and W.D. wrote the manuscript.

DECLARATION OF INTERESTS

The authors declare no competing interests.

REFERENCES

1. Pu, W., Li, J., Zheng, Y., Shen, X., Fan, X., Zhou, J.K., He, J., Deng, Y., Liu, X., Wang, C., et al. (2018). Targeting Pin1 by inhibitor API-1 regulates microRNA biogenesis and suppresses hepatocellular carcinoma development. Hepatology *68*, 547–560.
2. Ko, E., Kim, J.S., Bae, J.W., Kim, J., Park, S.G., and Jung, G. (2019). SERPINA3 is a key modulator of HNRNP-K transcriptional activity against oxidative stress in HCC. Redox Biol. *24*, 101217.
3. Chen, M., Wei, L., Law, C.T., Tsang, F.H., Shen, J., Cheng, C.L., Tsang, L.H., Ho, D.W., Chiu, D.K., Lee, J.M., et al. (2018). RNA N6-methyladenosine methyltransferase-like 3 promotes liver cancer progression through YTHDF2-dependent posttranscriptional silencing of SOCS2. Hepatology *67*, 2254–2270.
4. Dong, L., Dong, Q., Chen, Y., Li, Y., Zhang, B., Zhou, F., Lyu, X., Chen, G.G., Lai, P., Kung, H.F., et al. (2018). Novel HDAC5-interacting motifs of Tbx3 are essential for the suppression of E-cadherin expression and for the promotion of metastasis in hepatocellular carcinoma. Signal. Transduct. Target. Ther. *3*, 22.
5. El-Serag, H.B., Siegel, A.B., Davila, J.A., Shaib, Y.H., Cayton-Woody, M., McBride, R., and McGlynn, K.A. (2006). Treatment and outcomes of treating of hepatocellular carcinoma among Medicare recipients in the United States: a population-based study. J. Hepatol. *44*, 158–166.
6. Sun, D., Tan, S., Xiong, Y., Pu, W., Li, J., Wei, W., Huang, C., Wei, Y.Q., and Peng, Y. (2019). MicroRNA biogenesis is enhanced by liposome-encapsulated Pin1 inhibitor in hepatocellular carcinoma. Theranostics *9*, 4704–4716.
7. Berman, A.J., Akiyama, B.M., Stone, M.D., and Cech, T.R. (2011). The RNA accordion model for template positioning by telomerase RNA during telomeric DNA synthesis. Nat. Struct. Mol. Biol. *18*, 1371–1375.
8. Chen, L., Roake, C.M., Freund, A., Batista, P.J., Tian, S., Yin, Y.A., Gajera, C.R., Lin, S., Lee, B., Pech, M.F., et al. (2018). An activity switch in human telomerase based on RNA conformation and shaped by TCAB1. Cell *174*, 218–230.
9. Daniel, M., Peek, G.W., and Tollefsbol, T.O. (2012). Regulation of the human catalytic subunit of telomerase (hTERT). Gene *498*, 135–146.
10. Roake, C.M., and Artandi, S.E. (2020). Regulation of human telomerase in homeostasis and disease. Nat. Rev. Mol. Cell Biol. *21*, 384–397.
11. Jiang, J., Wang, Y., Sušac, L., Chan, H., Basu, R., Zhou, Z.H., and Feigon, J. (2018). Structure of telomerase with telomeric DNA. Cell *173*, 1179–1190.
12. Fell, V.L., and Schild-Poulter, C. (2015). The Ku heterodimer: function in DNA repair and beyond. Mutat. Res. Rev. Mutat. Res. *763*, 15–29.
13. Lobbardi, R., Pinder, J., Martinez-Pastor, B., Theodorou, M., Blackburn, J.S., Abraham, B.J., Namiki, Y., Mansour, M., Abdelfattah, N.S., Molodtsov, A., et al. (2017). TOX regulates growth, DNA repair, and genomic instability in T-cell acute lymphoblastic leukemia. Cancer Discov. *7*, 1336–1353.
14. Tong, W.M., Cortes, U., Hande, M.P., Ohgaki, H., Cavalli, L.R., Lansdorp, P.M., Haddad, B.R., and Wang, Z.Q. (2002). Synergistic role of Ku80 and poly (ADP-ribose) polymerase in suppressing chromosomal aberrations and liver cancer formation. Cancer Res. *62*, 6990–6996.
15. Wang, Y., Ghosh, G., and Hendrickson, E.A. (2009). Ku86 represses lethal telomere deletion events in human somatic cells. Proc. Natl. Acad. Sci. U S A *106*, 12430–12435.
16. Lipinska, N., Romaniuk, A., Paszel-Jaworska, A., Toton, E., Kopczynski, P., and Rubis, B. (2017). Telomerase and drug resistance in cancer. Cell. Mol. Life Sci. *74*, 4121–4132.
17. Sun, Y., He, L., Wang, T., Hua, W., Qin, H., Wang, J., Wang, L., Gu, W., Li, T., Li, N., et al. (2020). Activation of p62-Keap1-Nrf2 pathway protects 6-hydroxydopamine-induced ferroptosis in dopaminergic cells. Mol. Neurobiol. *57*, 4628–4641.
18. Ahmad, F., Dixit, D., Sharma, V., Kumar, A., Joshi, S.D., Sarkar, C., and Sen, E. (2016). Nrf2-driven TERT regulates pentose phosphate pathway in glioblastoma. Cell Death Dis. *7*, e2213.
19. Ruden, M., and Puri, N. (2013). Novel anticancer therapeutics targeting telomerase. Cancer Treat. Rev. *39*, 444–456.
20. Zhu, C.Q., Cutz, J.C., Liu, N., Lau, D., Shepherd, F.A., Squire, J.A., and Tsao, M.S. (2006). Amplification of telomerase (hTERT) gene is a poor prognostic marker in non-small-cell lung cancer. Br. J. Cancer *94*, 1452–1459.
21. Vinagre, J., Almeida, A., Pópulo, H., Batista, R., Lyra, J., Pinto, V., Coelho, R., Celestino, R., Prazeres, H., Lima, L., et al. (2013). Frequency of TERT promoter mutations in human cancers. Nat. Commun. *4*, 2185.
22. Liu, T., Li, W., Lu, W., Chen, M., Luo, M., Zhang, C., Li, Y., Qin, G., Shi, D., Xiao, B., et al. (2017). RBFOX3 promotes tumor growth and progression via hTERT signaling and predicts a poor prognosis in hepatocellular carcinoma. Theranostics *7*, 3138–3154.
23. Nemoz, C., Ropars, V., Frit, P., Gontier, A., Drevet, P., Yu, J., Guerois, R., Pitois, A., Comte, A., Delteil, C., et al. (2018). XLF and APLF bind Ku80 at two remote sites to ensure DNA repair by non-homologous end joining. Nat. Struct. Mol. Biol. *25*, 971–980.
24. Lopez-Gonzalez, R., Yang, D., Pribadi, M., Kim, T.S., Krishnan, G., Choi, S.Y., Lee, S., Coppola, G., and Gao, F.B. (2019). Partial inhibition of the overactivated Ku80-dependent DNA repair pathway rescues neurodegeneration in C9ORF72-ALS/FTD. Proc. Natl. Acad. Sci. U S A *116*, 9628–9633.
25. Walker, J.R., Corpina, R.A., and Goldberg, J. (2001). Structure of the Ku heterodimer bound to DNA and its implications for double-strand break repair. Nature *412*, 607–614.
26. Sato, H., Niimi, A., Yasuhara, T., Permata, T., Hagiwara, Y., Isono, M., Nuryadi, E., Sekine, R., Oike, T., Kakoti, S., et al. (2017). DNA double-strand break repair pathway regulates PD-L1 expression in cancer cells. Nat. Commun. *8*, 1751.
27. Ma, Q., Li, P., Xu, M., Yin, J., Su, Z., Li, W., and Zhang, J. (2012). Ku80 is highly expressed in lung adenocarcinoma and promotes cisplatin resistance. J. Exp. Clin. Cancer Res. *31*, 99.
28. Causse, S.Z., Marcion, G., Chanteloup, G., Uyanik, B., Boudesco, C., Grigorash, B.B., Douhard, R., Dias, A., Dumetier, B., Dondaine, L., et al. (2019). HSP110 translocates to the nucleus upon genotoxic chemotherapy and promotes DNA repair in colorectal cancer cells. Oncogene *38*, 2767–2777.
29. Herbert, K., Binet, R., Lambert, J.P., Louphrasitthiphol, P., Kalkavan, H., Sesma-Sanz, L., Robles-Espinoza, C.D., Sarkar, S., Suer, E., Andrews, S., et al. (2019). BRN2

suppresses apoptosis, reprograms DNA damage repair, and is associated with a high somatic mutation burden in melanoma. Genes Dev. *33*, 310–332.

30. Zang, Y., Pascal, L.E., Zhou, Y., Qiu, X., Wei, L., Ai, J., Nelson, J.B., Zhong, M., Xue, B., Wang, S., et al. (2018). ELL2 regulates DNA non-homologous end joining (NHEJ) repair in prostate cancer cells. Cancer Lett. *415*, 198–207.

31. Liu, E.S., and Lee, A.S. (1991). Common sets of nuclear factors binding to the conserved promoter sequence motif of two coordinately regulated ER protein genes, GRP78 and GRP94. Nucleic Acids Res. *19*, 5425–5431.

32. Kim, E., Li, K., Lieu, C., Tong, S., Kawai, S., Fukutomi, T., Zhou, Y., Wands, J., and Li, J. (2008). Expression of apolipoprotein C-IV is regulated by Ku antigen/peroxisome proliferator-activated receptor gamma complex and correlates with liver steatosis. J. Hepatol. *49*, 787–798.

33. Grote, J., König, S., Ackermann, D., Sopalla, C., Benedyk, M., Los, M., and Kerkhoff, C. (2006). Identification of poly (ADP-ribose) polymerase-1 and Ku70/Ku80 as transcriptional regulators of S100A9 gene expression. Bmc Mol. Biol. *7*, 48.

34. Shi, L., Qiu, D., Zhao, G., Corthesy, B., Lees-Miller, S., Reeves, W.H., and Kao, P.N. (2007). Dynamic binding of Ku80, Ku70 and NF90 to the IL-2 promoter in vivo in activated T-cells. Nucleic Acids Res. *35*, 2302–2310.

35. Mayeur, G.L., Kung, W.J., Martinez, A., Izumiya, C., Chen, D.J., and Kung, H.J. (2005). Ku is a novel transcriptional recycling coactivator of the androgen receptor in prostate cancer cells. J. Biol. Chem. *280*, 10827–10833.

36. Xiao, Y., Wang, J., Qin, Y., Xuan, Y., Jia, Y., Hu, W., Yu, W., Dai, M., Li, Z., Yi, C., et al. (2015). Ku80 cooperates with CBP to promote COX-2 expression and tumor growth. Oncotarget *6*, 8046–8061.

37. Liu, T., Jin, L., Chen, M., Zheng, Z., Lu, W., Fan, W., Li, L., Zheng, F., Zhu, Q., Qiu, H., et al. (2019). Ku80 promotes melanoma growth and regulates antitumor effect of melatonin by targeting HIF1-αdependent PDK-1 signaling pathway. Redox Biol. *25*, 101197.

38. Dinkova-Kostova, A.T., Holtzclaw, W.D., Cole, R.N., Itoh, K., Wakabayashi, N., Katoh, Y., Yamamoto, M., and Talalay, P. (2002). Direct evidence that sulfhydryl groups of Keap1 are the sensors regulating induction of phase 2 enzymes that protect against carcinogens and oxidants. Proc. Natl. Acad. Sci. U S A *99*, 11908–11913.

39. DeNicola, G.M., Karreth, F.A., Humpton, T.J., Gopinathan, A., Wei, C., Frese, K., Mangal, D., Yu, K.H., Yeo, C.J., Calhoun, E.S., et al. (2011). Oncogene-induced Nrf2 transcription promotes ROS detoxification and tumorigenesis. Nature *475*, 106–109.

40. Saito, T., Ichimura, Y., Taguchi, K., Suzuki, T., Mizushima, T., Takagi, K., Hirose, Y., Nagahashi, M., Iso, T., Fukutomi, T., et al. (2016). p62/Sqstm1 promotes malignancy of HCV-positive hepatocellular carcinoma through Nrf2-dependent metabolic reprogramming. Nat. Commun. *7*, 12030.

41. Li, J., Wang, Q., Yang, Y., Lei, C., Yang, F., Liang, L., Chen, C., Xia, J., Wang, K., and Tang, N. (2019). GSTZ1 deficiency promotes hepatocellular carcinoma proliferation via activation of the KEAP1/NRF2 pathway. J. Exp. Clin. Cancer Res. *38*, 438.

42. Angulo, J., El, A.M., Sevilleja-Ortiz, A., Fernández, A., Sánchez-Ferrer, A., Romero-Otero, J., Martínez-Salamanca, J.I., La Fuente, J.M., and Rodríguez-Mañas, L. (2019). Short-term pharmacological activation of Nrf2 ameliorates vascular dysfunction in aged rats and in pathological human vasculature. A potential target for therapeutic intervention. Redox Biol. *26*, 101271.

43. Guo, H., Xu, J., Zheng, Q., He, J., Zhou, W., Wang, K., Huang, X., Fan, Q., Ma, J., Cheng, J., et al. (2019). NRF2 SUMOylation promotes de novo serine synthesis and maintains HCC tumorigenesis. Cancer Lett. *466*, 39–48.